J. Earth Syst. Sci. (2020)129 51
https://doi.org/10.1007/s12040-019-1320-5

Observations of carbon dioxide and turbulent fluxes during fog conditions in north India

M N Patil[1,*], T Dharmaraj[1], R T Waghmare[1], Surender Singh[2], Prakash Pithani[1,3], Rachana Kulkarni[1,4], Narendra Dhangar[1,3], Devendraa Siingh[1], G R Chinthalu[1], Raj Singh[2] and Sachin Ghude[1]

[1]*Indian Institute of Tropical Meteorology, Pune 411 008, India.*
[2]*Ch Charan Singh Haryana Agricultural University, Hisar, Haryana 125 004, India.*
[3]*Department of Meteorology and Oceanography, Andhra University, Visakhapatnam, India.*
[4]*Savitribai Phule Pune University, Pune, India.*
**Corresponding author. e-mail: patil@tropmet.res.in*

MS received 27 July 2018; revised 15 September 2019; accepted 24 October 2019

The occurrence of thick fog for longer duration in the northern regions of India disturbs the aviation, road transportation and other day to day activities. To understand the turbulence properties during fog period, we measured the atmospheric turbulent parameters along with carbon dioxide concentrations in the atmospheric boundary layer using eddy covariance system. These measurements were conducted over the agricultural station, Hisar, India, during the months of January–February of the year 2017 and 2018. During this period, total five thick fog events and three moderate fog events were captured. The turbulent parameter such as friction velocity, stability, sensible and latent heat fluxes are presented with respect to fog events. During the study period, the western disturbance persists over the north Pakistan and neighborhood region which advects the large amount of moisture into the lower troposphere and further through evaporation. It enforces stable and clear sky atmospheric conditions and reduces the surface temperature leading to the formation of strong surface-based temperature inversion which facilitates the fog formation in the study region. The land surface processes with neutral stability conditions in the surface layer, play significant role to sustain fog in the study region. The observations show substantial increase of carbon dioxide concentration during the thick fog events. The foggy days did not depict the diurnal pattern in flux of CO_2. The anomalies of the meteorological parameters during foggy days and clear sky are analyzed. The foggy conditions (04:00–10:00 h, IST) are found to be characterized with low wind speed, high relative humidity with remarkable fluctuations in dew point temperature. Also, the sensible and latent heat flux shows remarkable changes during foggy and clear sky conditions.

Keywords. Carbon dioxide; atmospheric boundary layer stability; surface heat flux; wind speed; winter fog.

1. Introduction

The formation of thick fog extending over thousands of kilometers is the major weather hazards in South Asia as it disturbs the aviation and transportation activities and is also responsible for health issues. In the winter season (December–February), fog events occur in the northern part of India during the period of late night to early morning hours. The fog layer normally varies in

Published online: 21 January 2020

depth, from the lower few tens of meters to few hundred meters. Recently, it is observed that there has been a tremendous increase in the fog formation over northern parts of India, i.e., over Indo-Gangetic plain (Singh and Kant 2006; Srivastava *et al.* 2016). However, in other part of the world, a decreasing trend in fog frequency has been observed. In the regions including southeastern USA (Forthun *et al.* 2006), California (Johnstone and Dawson 2010), Europe (Vautard *et al.* 2009; van Oldenborgh *et al.* 2010, Avotniece *et al.* 2015) and south Korea (Belorid *et al.* 2015), the decrease in the fog intensity events are observed. This could be due to the rapidly expanding urban areas, which can be linked to the urban heat island effect and land cover change (Sachweh and Koepke 1995). The additional heat in urban areas increases the air temperature and reduces the cooling rates during the night. Moreover, the heat island effect appears mostly during nights with clear sky and calm winds (Kim and Baik 2004). It is shown that the climatic effect of urbanization is favorable to the fog formation in the nearby rural area but decreasing fog frequency within the urban area (Sachweh and Koepke 1997). Based on satellite data and meteorological parameters, Wang *et al.* (2010) have found that distribution of radiation fog depends on types of surface underneath.

The formation of fog is possible by three different processes: (a) cooling, (b) increase of moisture content, and (c) accumulation of hygroscopic aerosol particles. Fog over the flat terrain is formed mainly due to the radiational cooling at the earth's surface (radiation fog) and therefore has its maximum intensity in winter season (Sachweh and Koepke 1995). The radiation fog usually forms near the surface under clear skies in stagnant air associated with anticyclonic conditions after nocturnal surface cooling and temperature decrease to the dew point temperature (Welch *et al.* 1986; Gultepe *et al.* 2007). Thus, the basic requirement for the formation of radiation fog is high relative humidity, clear sky conditions and light winds. The high concentrations of aerosol particles in the boundary layer enhances the formation and persistence of fog by additional condensation nuclei (Srivastava *et al.* 2016).

Over northern India, the fog formation is mostly due to radiative cooling but, advection fog has also been observed (Dutta 2010). In the northern India, over Delhi, the fall in average maximum temperature by 2–3°C and increase in average fog hours in a day by 8 h was observed since 1989–2007 (Jenamani 2007). As far as turbulence in the atmospheric boundary layer is concerned, the collapse of turbulence was a necessity for the formation of fog, and moderate turbulence was favorable to the development and maintenance of fog (Ye *et al.* 2015). In the stable boundary layer, the pollutants are accumulated at the surface and it starts dispersing with the increase in radiation during daytime. This increases the radiative forcing leading to enhanced fog activity in winters (Tyagi *et al.* 2017). The observations presented in this analysis are from the rural agricultural environment. To develop better now-casting and forecasting of winter fog on various time and spatial scales, the Winter Fog Experiment (WIFEX) over the Indo-Gangetic Plains of India was planned (Ghude *et al.* 2017). This work analyses turbulence properties in the atmospheric boundary layer and surface meteorological conditions during fog events to improve our understanding of micro-physical process during fog occurrence. Also the carbon dioxide (CO_2) concentrations during the fog events have been quantified with the observations.

2. Experiment and observations

During the winter season, as a part of the Winter Fog Experiment (WIFEX) (Ghude *et al.* 2017), the Eddy Covariance (EC) system was installed (figure 1) over the station Hisar (29°10′N, 75°45′E, 215 m asl) in the northern India during January and February months of the year 2017 and 2018. The high frequency (10 Hz) measurements of wind, temperature, humidity and CO_2 were carried out using EC system (Patil *et al.* 2014, 2016). The EC system consists of the CO_2/H_2O open path gas analyser (Model LI-7500A by Licor Inc.) integrated with 3D sonic anemometer (Model Wind Master Pro by Gill Instruments). The wind and temperature as well as CO_2 and H_2O observations were sampled at 10 Hz. The complete description of both the sensors is given in table 1. The EC system was mounted on 10 m mast at a height of 6 m. The observational site was in the outskirt of the Hisar city, at a distance of $\sim$10 km having rural characteristics.

3. Surface and large scale meteorological conditions and data analysis

During the period of observations mentioned above, five thick fog events (18–20 January 2017 and 28, 29 January 2018) and three moderate fog

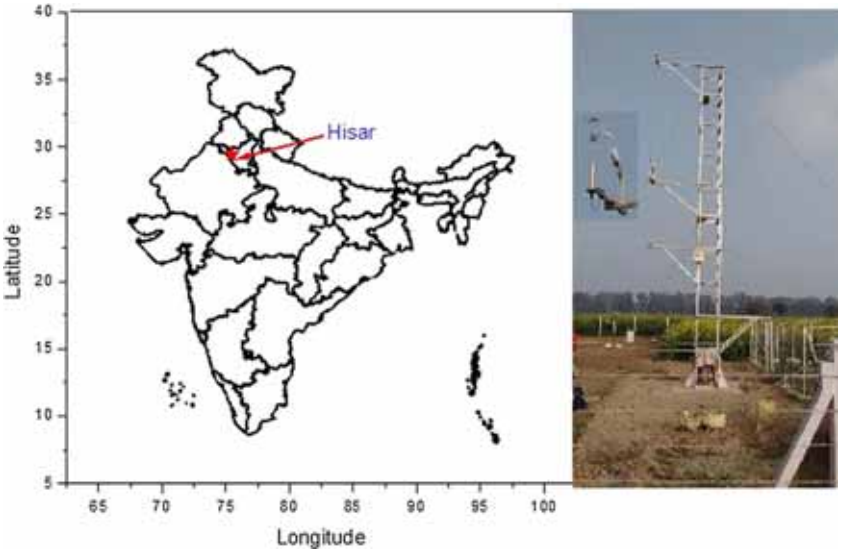

Figure 1. Location of Hisar site and Eddy covariance system installed at 6 m height on tower.

Table 1. Specification of Eddy covariance system installed during fog experiment at Hisar.

CO_2/H_2O gas analyser-Model LI-7500A	3D sonic anemometer-Model WindPro
Type Absolute, open-path, non-dispersive infrared gas analyser Detector Thermo-electrically cooled lead selenide Output rate 5, 10, or 20 Hz, software selectable Path Length 12.5 cm Calibration range For CO_2: 0–3000 ppm For H_2O: 0–60 ppt Accuracy For CO_2: within 1% of reading For H_2O: within 2% of reading Zero drift (per °C) For CO_2: ± 0.1 ppm typical; ± 0.3 ppm max. For H_2O: ± 0.03 ppt typical; ± 0.05 ppt max.	Outputs *Output rate*: 1, 2, 4, 8, 10, 16, 20, 32 Hz *Sample rate* (automatically selected): 20 or 32 Hz *Units of measure*: m/s, mph, KPH, knots, ft/min *Averaging*: Flexible 0–3600 s Wind speed *Range*: 0–65 m/s *Resolution*: 0.01 or 0.001 m/s *Accuracy (12 m/s) (Standard)**: <1.5% RMS *Accuracy (12 m/s) (to special order)* #*: < 1.0% RMS Wind direction *Range*: 0–359.9 *Resolution*: 1 or 0.1 *Accuracy (12 m/s) (Standard)**: 2 *Accuracy (12 m/s) (to special order)* #*: 0.5 Speed of sound *Range* 300–370 m/s *Resolution*: 0.01 m/s *Accuracy*: < ± 0.5% @20°C *Sonic temperature range*: − 40°C to + 70°C

events (30, 31 January 2018 and 1 February 2018) are considered in this study. Thick fog and moderate fog events were classified based on the visibility criteria only. Surface level meteorological parameters recorded during thick fog, moderate fog, clear sky and cloudy conditions are summarized in table 2. The rainfall occurred on 22 January (3.6 mm), 26 January (9.5 mm), 27 January (21.5 mm) of 2017 and 24 January (10.9 mm) and 13 February (1.2 mm) of 2018.

According to the daily and weekly weather reports by India Meteorological Department, the

western disturbance (WD) as a trough in mid- and upper-tropospheric westerlies was laying as an upper air circulation over north Pakistan and neighbourhood extending between 3.1 and 5.8 km above sea level (asl) with trough aloft running roughly along long. 66°E to the north of lat. 25°N on 17th January 2017. An induced circulation extending up to 1.5 km asl lies over Punjab and neighbourhood. On 18th January 2017, under the influence of WD the induced cyclonic circulation extending up to 1.5 km asl over Punjab and neighbourhood shifted over Haryana and adjoining Punjab. Severe cold wave conditions prevailed at isolated places over east and west Rajasthan. Night temperature was appreciably below normal in some parts of Haryana, Chandigarh and Delhi. WD induced cyclonic circulation extending up to 1.5 km asl continue to lay over Haryana and adjoining Punjab up to 25th January 2017. Dense fog with visibility ≤200 m occurred at a few places over Punjab and at isolated places over Jammu and Kashmir and west Rajasthan and shallow to moderate fog with visibility ≤500 m occurred at isolated places over Uttar Pradesh and Haryana, Chandigarh and Delhi in the morning hours under the influence of induced cyclonic circulation over northwest Rajasthan and adjoining areas of Haryana and Punjab. On 18th January 2017, thick fog with visibility ≤200 m occurred at a few places over Uttar Pradesh, Uttarakhand, Haryana, Chandigarh and Delhi. Shallow to moderate fog with visibility ≤500 m occurred at a few places over Uttar Pradesh, Haryana, Chandigarh and Delhi on 21–22 January 2017. Night temperature was below normal in some parts of Uttar Pradesh, Haryana, Chandigarh and Delhi. Dense fog with visibility ≤200 m occurred at a few places over Haryana, Chandigarh and Delhi.

During 25–31 January 2018, dense to very dense fog was observed at many places over Punjab, Haryana, Chandigarh, Delhi, Uttar Pradesh, and Bihar, at a few places over northwest Rajasthan and Sub Himalayan West Bengal and at isolated places over Assam, Meghalaya and Nagaland, Manipur, Mizoram and Tripura on one or two days during the week. Cold wave conditions were observed at isolated places over Vidarbha, southern parts of east Madhya Pradesh and northern parts of Rajasthan, Punjab, Haryana and Odisha on a few days and over East Uttar Pradesh, Bihar, west Madhya Pradesh, Himachal Pradesh, Uttarakhand, Marathwada and Sub Himalayan West Bengal for one to two days. The lowest minimum temperature of 2.0°C was recorded at Bhilwara (Rajasthan) in the plains of the country on 25th January 2018. The trough persisted over the same region with the embedded cyclonic circulation extending up to 3.1 km amsl on 28th January 2018. It lay over Equatorial Indian Ocean and adjoining South West Bay of Bengal with the embedded cyclonic circulation extending up to 1.5 km asl on 29th January 2018. It lay over Equatorial Indian Ocean and adjoining southwest Bay of Bengal off south Sri Lanka coast with the embedded cyclonic circulation extending up to 0.9 km asl on 30th and 31st January 2018. The minimum temperature was below normal on 28 and 29 January 2018, but it was normal on 30 and 31 January 2018.

Table 2. *Surface meteorological conditions during thick fog, moderate fog, cloudy and clear sky conditions over Hisar.*

	Sky conditions				Air temperature		Wind speed
Date	Fog intensity	Bright sunshine (h)	Visibility at 02 UTC (m)	Evaporation mm day^{-1}	Min (K)	Max (K)	average (Km h^{-1})
17 Jan 2017	Cloudy	3.1	< 1000	1.0	275.0	286.1	4.4
18 Jan 2017	Thick	3.6	< 20	1.2	275.4	292.4	2.3
19 Jan 2017	Thick	5.6	< 20	1.4	279.4	292.5	3.2
20 Jan 2017	Thick	7.0	< 50	1.0	276.1	293.3	2.7
21 Jan 2017	Cloudy	4.9	< 1000	1.2	276.7	292.1	2.0
24 Feb 2017	Clear	10.0	< 1000	3.3	282.4	299.1	2.6
25 Feb 2017	Clear	9.8	< 1000	2.9	282.0	301.0	3.7
26 Feb 2017	Clear	9.8	< 1000	2.7	282.5	299.8	2.8
28 Jan 2018	Thick	4.1	< 3	0.6	291.1	278.9	1.4
29 Jan 2018	Thick	4.0	< 3	0.6	291.1	278.7	0.7
30 Jan 2018	Moderate	5.7	< 500	0.9	297.2	278.2	1.1
31 Jan 2018	Moderate	7.3	< 500	1.9	297.6	280.7	1.8
1 Feb 2018	Moderate	7.8	< 500	1.6	297.2	280.7	2.1

The observations collected at 10 Hz for 30 min durations were stored in a single data file which consisted of 18,000 sample points. Each data file is processed separately. All the observations of CO_2 and water vapour during the rainfall and whenever relative humidity exceeded 90% were discarded. The observations were processed using EddyPro program supplied by the Licor Inc. In the EddyPro program, the natural wind coordinates were rotated for minimizing the effect of vibrations and deviation of the sensors according to Lee *et al.* (2004); WPL correction for density effects due to heat and water vapour transfer (Webb *et al.* 1980) and data quality control test for steady state and integral turbulence characteristics (Foken and Wichura 1996) were adopted in the analysis.

4. Results and discussion

4.1 *Mechanism of the fog formation*

As reported in the large scale meteorological conditions in earlier section, the western disturbance (WD) was persisting over the region of north Pakistan and neighbourhood during the study period of 2017 and 2018. WD causes light to moderate spells of rainfall over the northern region during winter (Dimri *et al.* 2015) which advects large amount of moisture into the lower troposphere and further through evaporation. In addition, irrigation for winter crops and the irrigation network in this region add significant amount of moisture into the lower atmosphere (Badarinath *et al.* 2009). As soon as the lower-level ridge line forms over the northern region, it enforces persisting stable (calm winds) and clear atmosphere conditions and lower surface temperature leading to the formation of strong surface-based inversions. These conditions facilitate fog formation and its sustainment in the area (Jenamani 2007; Sawaisarje *et al.* 2014). The land surface processes and emission sources in the Indo-Gangetic Plains (IGP) region contribute to moisture supply and high concentrations of pollutants (Kulkarni *et al.* 2009; Ghude *et al.* 2010) which favour the persistence of hazy/foggy conditions for extended periods. Sensitivity studies carried out by chemistry transport model show that organic compounds, secondary aerosols and inorganic gaseous precursors have substantial impact on the fog formation process and microphysical structure of the fog event (Xing-Can and Xue-Liang 2012).

4.2 *Diurnal variation of CO_2 and relative humidity*

The measurement of CO_2 concentration in the fog environment especially during dense fog hours is not yet reported from Indian subcontinent. In the observations presented in this study, on the days of clear sky and moderate fog, the CO_2 concentration was ranging from $\sim$380 ppm (minimum) in the evening hours to $\sim$420 ppm (maximum) in the morning hours. During thick fog events, the CO_2 concentration was significantly increased to 740 ppm on 18 January 2017, 780 ppm on 29 January 2018 and 840 ppm on 30 January 2018. This increase was nearly two times than the normal concentration. The maximum concentration was occurred at nearly midnight to early morning hours (figure 2a and i). Similarly the relative humidity observed during above events is shown in figure 2(c and j) and it was above 80%. The studies on CO_2 concentration during the foggy weather are not yet reported from Indian subcontinent and hence are not available for comparison. To compare the CO_2 concentrations during thick fog events, we analyzed the observations from Delhi station which is at $\sim$160 km from Hisar in south-east direction. Figure 3 shows the daily anomaly in CO_2 mixing ratio during 17–25 January, 2017 and during 28 January–1 February 2018 over Hisar and during 24–28 January 2018 over New Delhi. During the thick fog days, the mixing ratios of CO_2 increased remarkably by $\sim$36.2 ppb and 15.7 ppb at Hisar and Delhi stations, respectively. The mean of the CO_2 mixing ratio for the period considered for Hisar in 2017 and 2018 are 399.2 and 441.5, respectively, while it is 459.3 for Delhi in 2018.

4.3 *Diurnal variation of surface meteorological parameters*

The analysis of diurnal pattern of meteorological parameter (temperature, humidity, wind speed, wind direction, etc.) helps us to better understand the micro-physical processes which are important for formation, maintenance and dissipation of fog. In the early morning hours when fog occurred, the boundary layer can be under stable stratification and the pollutants were trapped in the boundary layer due to the absence of adequate turbulence to disperse the pollutants. The clear sky, low winds, high relative humidity and low air temperature are the necessity for the formation of radiation fog. The observed air temperature (figure 2c and k) at

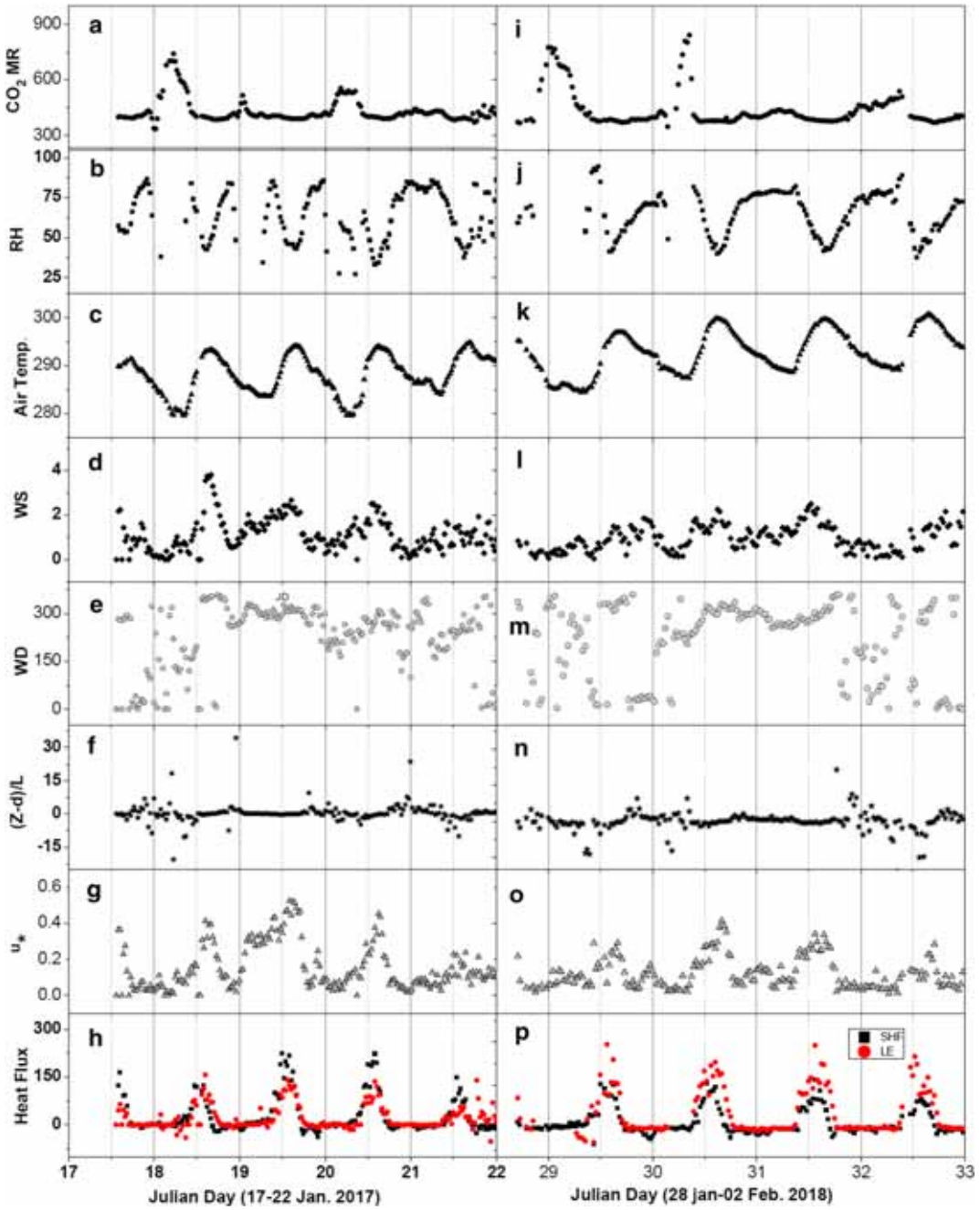

Figure 2. Day-to-day variation during 17–22 January 2017 of (**a**) CO_2 mixing ratio in ppm, (**b**) relative humidity in percentage (%), (**c**) air temperature in °K, (**d**) wind speed in m s^{-1}, (**e**) wind direction in degree, (**f**) dimensionless Monin–Obukhov length scale $(z - d)/L$, (**g**) friction velocity in m s^{-1}, (**h**) sensible and latent heat flux in W m^{-2}. Day to day variation during 28 January–2 February 2018 of (**i**) CO_2 mixing ratio in ppm, (**j**) relative humidity in percentage (%), (**k**) air temperature in °K, (**l**) wind speed in m s^{-1}, (**m**) wind direction in degree, (**n**) dimensionless Monin–Obukhov length scale $(z - d)/L$, (**o**) friction velocity in m s^{-1}, and (**p**) sensible and latent heat flux in W m^{-2}.

6 m was ranging from 279–301 K, whereas wind speed (figure 2d and l) was ranging from nearly 0–4 m s^{-1}. The wind speed was lower (mostly < 0.5 m s^{-1}) during evening to midnight hours, i.e., at the time of fog formation. The wind speed was maximum in the afternoon hours which contributes for the mixing and dispersion of fog. The wind direction observations at 6 m are shown in figure 2(e and m). On clear and cloudy sky conditions, the wind direction was confined to north, north-west and west. But during the onset of moderate fog and thick fog period, it extends to almost all the sectors of wind direction. Ye *et al.* (2015) investigated the vertical structure of

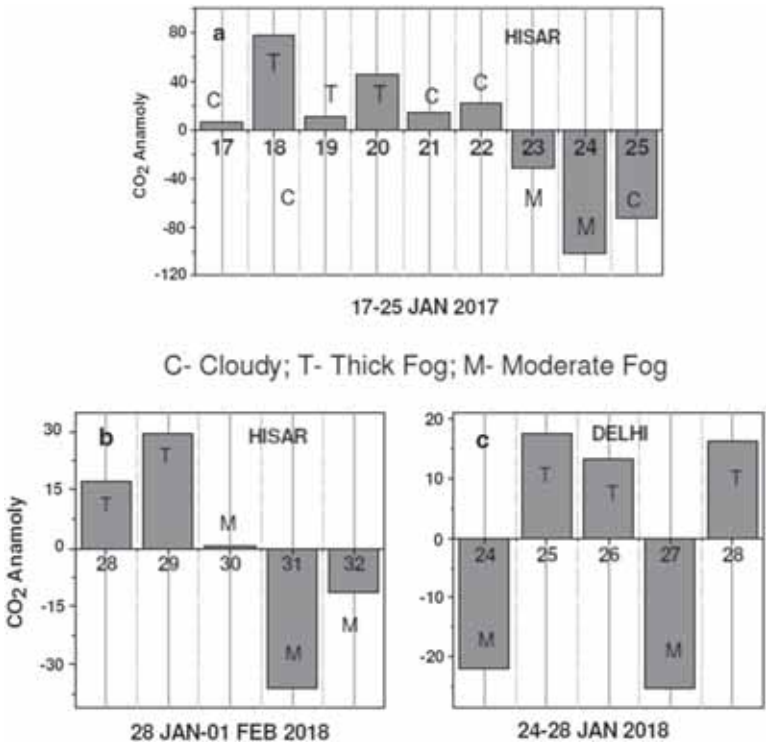

Figure 3. Daily Anomoly in CO_2 mixing ratio in ppm (**a**) 17–25 January, 2017 for Hisar, (**b**) 28 January–1 February, 2018 for Hisar, and (**c**) 24–28 January 2018 for Delhi. The CO_2 observations are taken half hourly and thus, 48 data samples are available to calculate the daily mean. The zero line is the mean of observations for the period indicated in each figure.

turbulence in fog events over the Tianjin area of north China and found that the fog events were characterized by low wind speed throughout the fog layer. The long-term trend of fog frequency in the Belgrade region (Serbia) shows that over a station Belgrade-Vračar, fog occurred most frequently in stable anticyclonic weather with light winds (Vujović and Todorović 2018). The observations at the Lisbon airport (Portugal) shows the change in wind direction and low wind speed at the time of onset of radiation fog, and the air temperature at 2 m was ranging from 275 to 288 K during the fog period (Belo-Pereira and Santos 2016). Thus, weak wind during the fog period observed in this study is corroborating the studies from other regions. According to Ye *et al.* (2015), the increase in wind speed, turbulence intensity and short-wave radiation may lead to the dissipation of fog.

4.4 *The characteristics of turbulence during the fog events*

In this section, we present the surface layer turbulent parameters such as stability (Monin–Obukhov length scale), friction velocity and surface heat fluxes. These turbulent parameters are computed using Eddy covariance method. The diurnal variations of surface layer stability (figure 2f and n) and friction velocity (figure 2g and o) over Hisar are presented. The friction velocity was greater on clear sky conditions (0.01–0.6 m s^{-1}) which reduced to 0.01–0.4 m s^{-1} in foggy conditions. The friction velocity was weak after sunset in the evening hours to the midnight hours, ranging from 0.05–0.15 m s^{-1} indicating weak turbulence during the formation stage of fog (figure 2g and o). The friction velocity increased up to 0.5 m s^{-1} in the afternoon hours. During the onset of fog (around evening hours after sunset to the midnight hours), the boundary layer was stable as indicated by positive values of $(z - d)/L$ shown in figure 2(f and n). Later, after the midnight to early morning hours, the boundary layer was nearly stable to near neutral (moderate turbulence) and it became unstable during daytime. The diurnal stability pattern was observed to be similar in thick as well as moderate fog events. Thus, the weak turbulence was observed during the formation of fog, later the boundary layer became neutral (moderate turbulence) to maintain the fog in the boundary layer. A study by Ye *et al.* (2015) from the rural environment also shows that in the atmospheric boundary layer, the collapse of turbulence was a necessity for the

formation of fog, and moderate turbulence was favourable to the development and maintenance of fog. Also the higher aerodynamic roughness leads to improved fog formation conditions due to the reduction of horizontal wind speed. On the other hand, higher urban temperatures and reduced moisture in the air will decrease fog probability (Sachweh and Koepke 1995). The results from the study (Terradellas *et al.* 2008) indicate that, before the formation of fog, the turbulence energy is much weaker near the ground than aloft, there is a strong inversion and an increase in specific humidity above the top of the fog layer. Figure 2(h and p) shows the observed fluxes of sensible heat and latent heat during the foggy and cloudy days. In the afternoon hours, the latent heat flux goes up to 300 W m^{-2}, whereas sensible heat flux goes up to 225 W m^{-2}. In the fog events of 2018, in the afternoon hours, the latent heat flux was higher than the sensible heat flux, but in the events of the year 2017 (19–20 January 2017), sometimes sensible heat flux was higher than the latent heat flux. A study by Hao *et al.* (2017) over Tianjin, China observed that during fog and haze coexistence period, the sensible and latent heat flux (at 40, 100 and 200 m) was fluctuated significantly and the latent heat flux was greater than the sensible heat flux. We do not observe such fluctuations and the diurnal peak in sensible and latent heat fluxes in the afternoon hours is well marked. As stated above, the formation of strong surface-based inversions (stable conditions with downward sensible heat flux) facilitate fog formation and its sustainment in the observational area. In stable conditions, the turbulence in the boundary layer is weak. The atmospheric pollutants (including CO_2) are trapped in this stable layer. Due to the lack of solar heating, pollutants are unable to disperse from the surface layer and the concentration of CO_2 is increased at the surface. Once the solar heating increases, the dispersion of pollutants begins and a CO_2 concentration decreases at the surface.

4.5 *Characteristics of CO_2 flux during foggy and clear sky days*

Figure 4 shows the diurnal variation of CO_2 flux during foggy and clear sky conditions. These fluxes were computed from the high resolution observations (10 Hz) of CO_2 and wind components using the Eddy-pro program supplied by LICOR Inc. The diurnal pattern of the CO_2 flux is more prominent during clear sky days. The foggy days did not depict the clear diurnal pattern because of the lack of solar radiation. The mean magnitude of the CO_2 flux during foggy hours (04–10 h) of days (18–20 January 2017) was 0.18 ± 6.45 μmol m^{-2} s^{-1} and the magnitude were ranging from –16.08 to 20.37 μmol m^{-2} s^{-1}. Similarly during the clear sky days (24–26 February, 2017), the mean magnitude of CO_2 flux during 04–10 h was 0.33 ± 4.09 μmol m^{-2} s^{-1} and the magnitude were ranging from −11.73 to 15.18 μmol m^{-2} s^{-1}. Thus no significant change in CO_2 flux was observed during fog hours. During the clear sky days, the measured fluxes showed a clear daily pattern correlated with diurnal stability. On the clear sky days, the CO_2 flux was observed to be negative (uptake) during daytime and positive in the night-time. Being a rural site, diurnal maxima was observed in the noon hours at 11–12 h IST when the intensity of solar radiation was high. Thus, a CO_2 uptake flux in the noon hours was greater due to the biogenic processes. Opposite to the observation during clear sky hours, CO_2 flux was observed to be positive during some foggy hours. This could be attributed to the insuffcient photosynthesis in the absence of intense solar radiation. During the non-rainy period of August 2011, over the Indian site of Mahabubnagar, Patil *et al.* (2014) reported the diurnal variation of CO_2 flux values in the range of −24.1 to 9.5 μmol m^{-2} s^{-1}. The magnitude of CO_2 fluxes reported in the above study corroborates with the magnitudes observed in this study. During daytime, Lohou *et al.* (2010) observed the CO_2 flux in range of −6 to −20 μmol m^{-2} s^{-1} in rainy season (May–September) over the tropical Nangatchori site in northern Benin, located in a Sudanian–Guinean vegetation-type area, surrounded by woodland, crops and fallow. Observed night-time flux in this study is comparable with the results by Lee and Hu (2002) over the mid-latitudinal region of mixed forest on non-flat terrain. They observed positive flux of CO_2 (>23 μmol m^{-2} s^{-1}) frequently at night hours. Kidston *et al.* (2010) observed the CO_2 flux in the range of −6 to 4 μmol m^{-2} s^{-1} in the summer season over Jack Pine forest of Canada.

4.6 *Observed fluctuations in boundary layer turbulence parameters during thick fog and clear sky conditions*

There was an increase in the CO_2 concentration during thick fog hours in the year of 2017 and 2018 over the station Hisar and New Delhi as shown in figure 3. In this section, we report the change in boundary layer parameters with respect to thick fog days and clear sky days. For the computation of

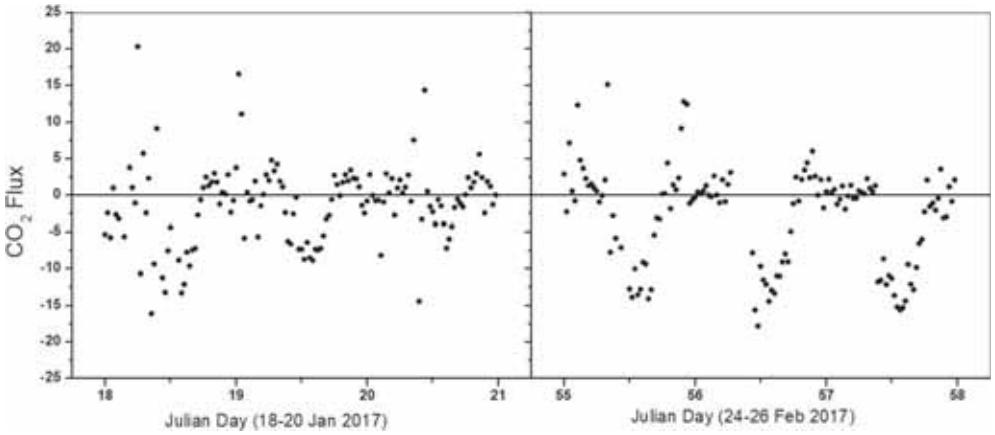

Figure 4. Diurnal variation of flux of CO_2 (μmol m^{-2} s^{-1}) observed during thick foggy days (18–20 January 2017) and clear sky days (24–26 February 2017) over Hisar.

anomalies in the boundary layer parameters, half hourly average of respective parameter of six days (mean of six data points for each half hour) is computed. It is seen from figure 5(a) that the CO_2 concentration was increased during thick fog conditions (18–20 January 2017) and remains at normal range during the clear sky conditions (24–26 February 2017). Relative humidity was higher in the morning to noon hours on foggy days (figure 5b). During clear sky days, the anomaly in air temperature and dew point temperature follows the uniform fluctuations but during the foggy days, remarkable fluctuation in dew point temperature is noticed (figure 5c). As seen in figure 5(d), the wind speed was low (as indicated by negative anomaly) during day time on foggy days whereas high (as indicated by positive anomaly) wind speed was observed during clear sky days (except on 25 February 2017). Friction velocity shows greater fluctuations during fog as well as clear sky days (figure 5e). On foggy days (18 and 20 January) during day time, the friction velocity was low; but on 19 January, it was high. Similarly, on clear sky days, during daytime, the friction velocity was high on 24 and 26 February; but it was low on 25 February. Remarkable changes are noticed on foggy and clear sky days. Figure 5(f) shows the anomaly in sensible heat flux and latent heat flux on foggy and clear sky days. The latent heat flux was low (indicated by negative anomaly) during daytime on foggy days whereas sensible heat flux was high (indicated by positive anomaly). The reverse anomaly was observed in clear sky days. Thus, the foggy conditions are characterized with low wind speed, high relative humidity with remarkable fluctuations in dew point temperature. Also, the sensible and latent heat flux shows remarkable changes during fog and clear sky days.

5. Summary and conclusions

In this paper, five thick fog and three moderate fog events that occurred in the winter of 2017 and 2018 were analyzed by using the eddy covariance measurements recorded at 6 m in the agricultural rural site in Hisar. The turbulence measurements by eddy covariance system (sonic anemometer and CO_2 and water vapour concentrations analyser) have been carried out. During the study period, the western disturbance persists over the north Pakistan and neighbourhood region which advects the large amount of moisture into the lower troposphere and further through evaporation. It enforces stable (calm winds) and clear sky atmospheric conditions and reduces the surface temperature leading to the formation of strong surface-based inversions which facilitate the fog formation in the study region. The analysis of these observations reveals the following conclusions:

- The concentration of CO_2 was increased substantially during the thick fog events. During thick foggy days, the surface temperature was decreased, the wind direction was not uniform and winds come almost from all the sectors (0–360°) of wind directions. The wind speed was low (<0.5 m s^{-1}) at the fog formation stage and it was maximum at the time of dissipation in the afternoon hours.

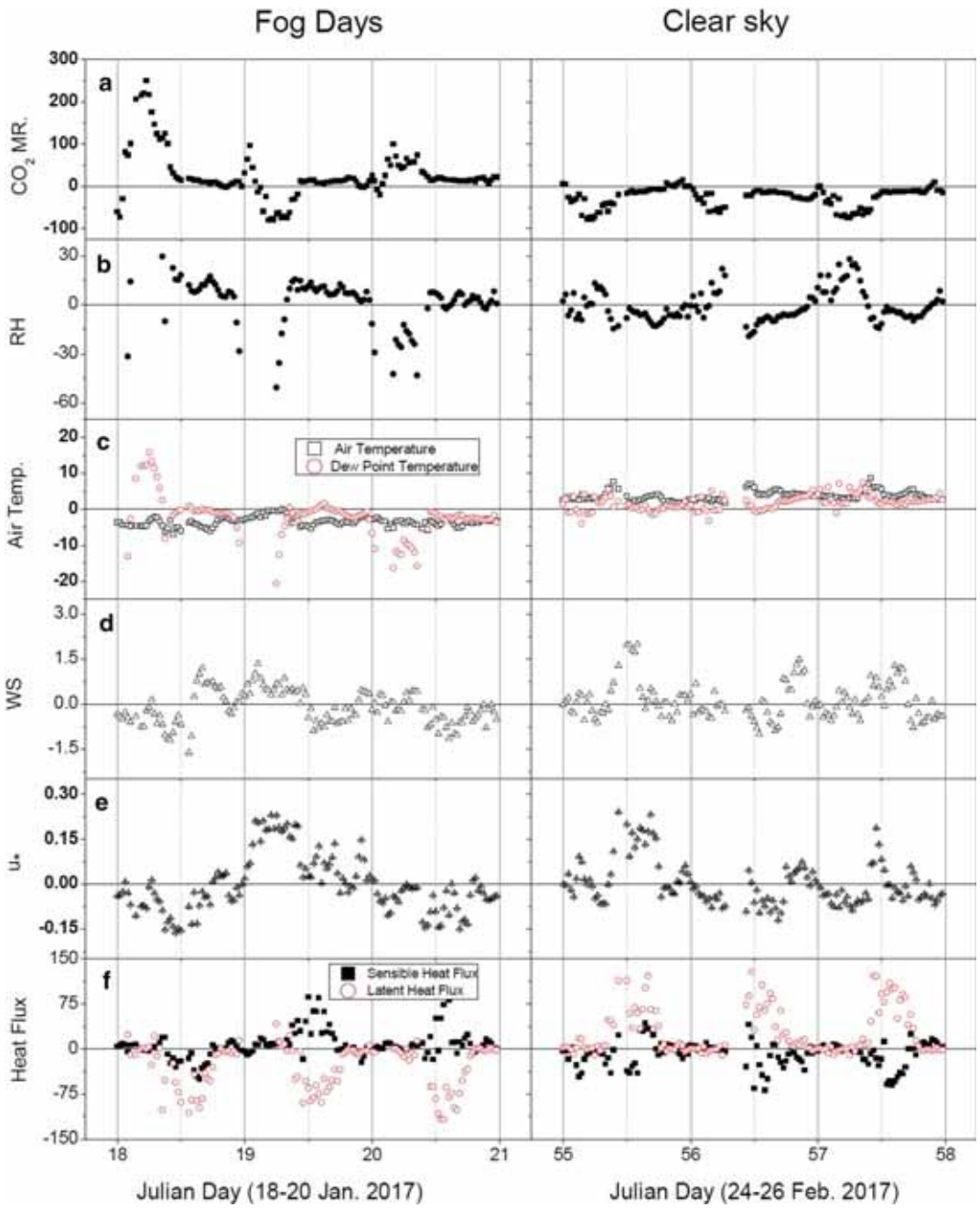

Figure 5. Anomaly observed during thick foggy days (18–20 January 2017) and clear sky days (24–26 February 2017) over Hisar for (**a**) CO_2 mixing ratio in ppm, (**b**) relative humidity in percentage (%), (**c**) air temperature and dew point temperature in degree Kelvin (K), (**d**) wind speed in m s^{-1}, (**e**) friction velocity in m s^{-1}, and (**f**) sensible and latent heat flux in W m^{-2}.

- The relative humidity was increased during and after the onset of fog, reaching to greater than 80%. During the dissipation stage of fog, the latent heat flux was in the range of 150–300 W m^{-2} and the sensible heat flux was in the range of 150–200 W m^{-2}.
- The weak turbulence was observed during the formation stage of fog. Later the boundary layer became neutral to maintain the fog. The fog is dissipated in the unstable boundary layer conditions.
- The foggy conditions are characterized with low wind speed, high relative humidity with remarkable fluctuations in dew point temperature. Also, the sensible and latent heat flux shows remarkable changes during fog and clear sky days.
- The diurnal cycle of CO_2 flux was more prominent on clear sky days. On foggy days, the

diurnal pattern is not clearly seen due to the absence of solar radiation.

Acknowledgements

The experiment is fully sponsored and funded by the Ministry of Earth Sciences (MoES), Government of India. We thank Dr M Rajeevan, the Secretary, MoES and Prof Ravi S Nanjundiah, the Director of Indian Institute of Tropical Meteorology (IITM), Pune for extending all the scientific, technical as well as financial support. We thank Airports Authority of India for providing logistic support and cooperation to conduct the experiment inside Indira Gandhi International Airport (IGIA), New Delhi. We also thank India Meteorological Department for support at IGIA New Delhi site and for providing daily and weekly weather reports. We acknowledge Mr Mahesh Darua, Mr Sanjay Thorat and IITM workshop team for erecting tower platform ready for the observations. We thank the Agro-Meteorology departmental staff of Choudhary Charansingh Agricultural University, Hisar for extending all the local and logistic support.

References

Avotniece Z, Klavins M and Lizuma L 2015 Fog climatology in Latvia; *Theor. Appl. Climatol.* **122** 97–109.

Badarinath K V S, Shailesh K K, Anu Rani S and Roy P S 2009 Fog over Indo-Gangetic plains – a study using multisatellite data and ground observations; *IEEE J. Sel. Top. Appl. Earth Obs. Remote Sens.* **2(3)** 185–195.

Belo-Pereira M and Santos J A 2016 A persistent wintertime fog episode at Lisbon airport (Portugal): Performance of ECMWF and AROME models; *Meteorol. Appl.* **23** 353–370.

Belorid M, Lee C B, Kim J C and Cheon T H 2015 Distribution and long-term trends in various fog types over South Korea; *Theor. Appl. Climatol.* **122** 699–710.

Dimri A P, Niyogi D, Barros A P, Ridley J, Mohanty U C, Yasunari T and Sikka D R 2015 Western disturbances: A review; *Rev. Geophys.* **53** 225–246. https://doi.org/10.1002/2014RG000460.

Dutta H N 2010 Acoustic sounding probing of fog dynamics, forecaster-users interactive workshop on fog monitoring and forecasting services 2010–2011, Dec. 2010.

Foken T and Wichura B 1996 Tools for quality assessment of surface-based flux measurements; *Agr. Forest Meteorol.* **78** 83–105.

Forthun G M, Johnson M B, Schmitz W G, Blume J and Caldwell R J 2006 Trends in fog frequency and duration in the southeast United States; *Phys. Geogr.* **27** 206–222.

Ghude S D, Bhat G S, Prabha T, Jenamani R K, Chate D M, Safai P D, Karipot A K, Konwar M, Pithani P, Sinha V, Rao P S P, Dixit S A, Tiwari S, Todekar K, Varpe S, Srivastava A K, Bisht D S, Murugavel P, Ali K, Mina U, Dharua M, Jaya Rao Y, Padmakumari B, Hazra A, Nigam N, Shende U, Lal D M, Acharja P, Kulkarni R, Subharthi C, Balaji B, Varghese M, Bera S and Rajeevan M 2017 Winter fog experiment over the Indo-Gangetic plains of India; *Curr. Sci.* **112** 767–784.

Ghude S D, Kulkarni P S, Beig G, Jain S L and Arya B C 2010 Global distribution of tropospheric ozone and its precursors: A view from space; *Int. J. Remote Sens.* **31(2)** 485–495.

Gultepe I, Tardif R, Michaelides S C, Cermak J, Bott A, Bendix J, Müller M D, Pagowski M, Hansen B, Ellrod G, Jacobs W, Toth G and Cober S G 2007 Fog research: A review of past achievements and future perspectives; *Pure Appl. Geophys.* **164(6–7)** 1121–1159.

Hao T, Han S, Chen S, Shan X, Zai Z, Qiu X, Yao Q, Liu J, Chen J and Meng L 2017 The role of fog in haze episode in Tianjin, China: A case study for November 2015; *Atmos. Res.* **194** 235–244.

Jenamani R K 2007 Alarming rise in fog and pollution causing a fall in maximum temperature over Delhi; *Curr. Sci.* **93** 314–322.

Johnstone J A and Dawson T E 2010 Climatic context and ecological implications of summer fog decline in the coast redwood region; *Proc. Natl. Acad. Sci.* **107** 4533–4538. https://doi.org/10.1073/pnas.0915062107.

Kidston J, Brümmer C, Black T A, Morgenstern K, Nesic Z, McCaughey J H and Barr A G 2010 Energy balance closure using eddy covariance above two different land surfaces and implications for CO_2 flux measurements; *Bound.-Layer Meteorol.* **136** 193–218.

Kim Y H and Baik J J 2004 Daily maximum urban heat island intensity in large cities of Korea; *Theor. Appl. Climatol.* **79** 151–164, https://doi.org/10.1007/s00704-004-0070-7.

Kulkarni P S, Jain S L, Ghude S D, Arya B C and Dubey P K 2009 On some aspects of tropospheric ozone variability over the Indo-Gangetic (IG) basin, India; *Int. J. Remote Sens.* **30(15–16)** 4111–4122.

Lee X and Hu X 2002 Forest-air fluxes of carbon, water and energy over non-flat terrain; *Bound.-Layer Meteorol.* **103** 277–301.

Lee X, Massman W and Law B (2004) Handbook of Micrometeorology: A Guide for Surface Flux Measurement and Analysis, Kluwer Academic Publishers, Dordrecht, pp. 60–61.

Lohou F, Said F, Lothon M, Durand P and Serca D 2010 Impact of boundary-layer processes on near-surface turbulence within the West African Monsoon; *Bound.-Layer Meteorol.* **136** 1–23.

Patil M N, Dharmaraj T, Waghmare R T, Prabha T V and Kulkarni J R 2014 Measurements of carbon dioxide and heat fluxes during monsoon-2011 season over rural site of India by eddy covariance technique; *J. Earth Syst. Sci.* **123** 177–185.

Patil M N, Waghmare R T, Dharmaraj T, Chinthalu G R, Devendraa Siingh and Meena G S 2016 The influence of wind speed on surface layer stability and turbulent fluxes over southern Indian peninsula station; *J. Earth Syst. Sci.* **125(7)** 1399–1411.

Sachweh M and Koepke R 1997 Fog Dynamics in an Urbanized Area; *Theor. Appl. Climatol.* **58** 87–93.

Sachweh M and Koepke R 1995 Radiation fog and urban climate; *Geophys. Res. Lett.* **22** 1073–1076.

Sawaisarje G K, Khare P, Shirke C V, Deepakumar S and Narkhede N M 2014 Study of winter fog over Indian subcontinent: Climatological perspectives; *Mausam* **65(1)** 19–28.

Singh J and Kant S 2006 Radiation fog over north India during winter from 1989–2004; *Mausam* **2** 271–290.

Srivastava S K, Sharma A R and Sachdeva K 2016 A ground observations based climatology of winter fog: Study over the Indo-Gangetic Plains, India; *Inter. J. Environ. Ecol. Eng.* **10(7)** 742–753.

Terradellas E, Ferreres E and Soler M R 2008 Analysis of turbulence in fog episodes; *Adv. Sci. Res.* **2** 31–34.

Tyagi S, Tiwari S, Mishra A, Singh S, Philip K Hopke, Surender Singh and Attri S D 2017 Characteristics of absorbing aerosols during winter foggy period over the National Capital Region of Delhi: Impact of planetary boundary layer dynamics and solar radiation flux; *Atmos. Res.* **188** 1–10.

van Oldenborgh G J, Yiou P and Vautard R 2010 On the roles of circulation and aerosols in the decline of mist and dense fog in Europe over the last 30 years; *Atmos. Chem. Phys.* **10** 4597–4609.

Vautard R, Yiou P and van Oldenborgh G J 2009 Decline of fog, mist and haze in Europe over the past 30 years; *Nat. Geosci.* **2** 115–119.

Vujović D and Todorović N 2018 Urban–rural fog differences in Belgrade area, Serbia; *Theor. Appl. Climatol.* **131** 889–898.

Wang J L, Li S M, Liu X L and Wu X J 2010 An analysis of the fog distribution in Beijing for the 2001–2005 period using NOAA and FY data; *Atmos. Res.* **96** 575–589.

Webb E K, Pearman G I and Leuning R 1980 Correction of the flux measurements for density effects due to heat and water vapour transfer; *Quart. J. R. Meteorol. Soc.* **106** 85–100.

Welch R M, Ravichandran M G and Cox S K 1986 Prediction of quasi-periodic oscillations in radiation fog. Part I: Comparison of simple similarity approaches; *J. Atmos. Sci.* **43(7)** 633–651.

Xing-Can and Xue-Liang 2012 Impacts of secondary aerosols on a persistent fog event in Northern China; *Atmos. Ocean. Sci. Lett.* **5(5)** 401–407.

Ye X, Wu B and Zhang H 2015 The turbulent structure and transport in fog layers observed over the Tianjin area; *Atmos. Res.* **153** 217–234.

Corresponding editor: Kavirajan Rajendran